Proteins at Interfaces
Physicochemical and Biochemical Studies

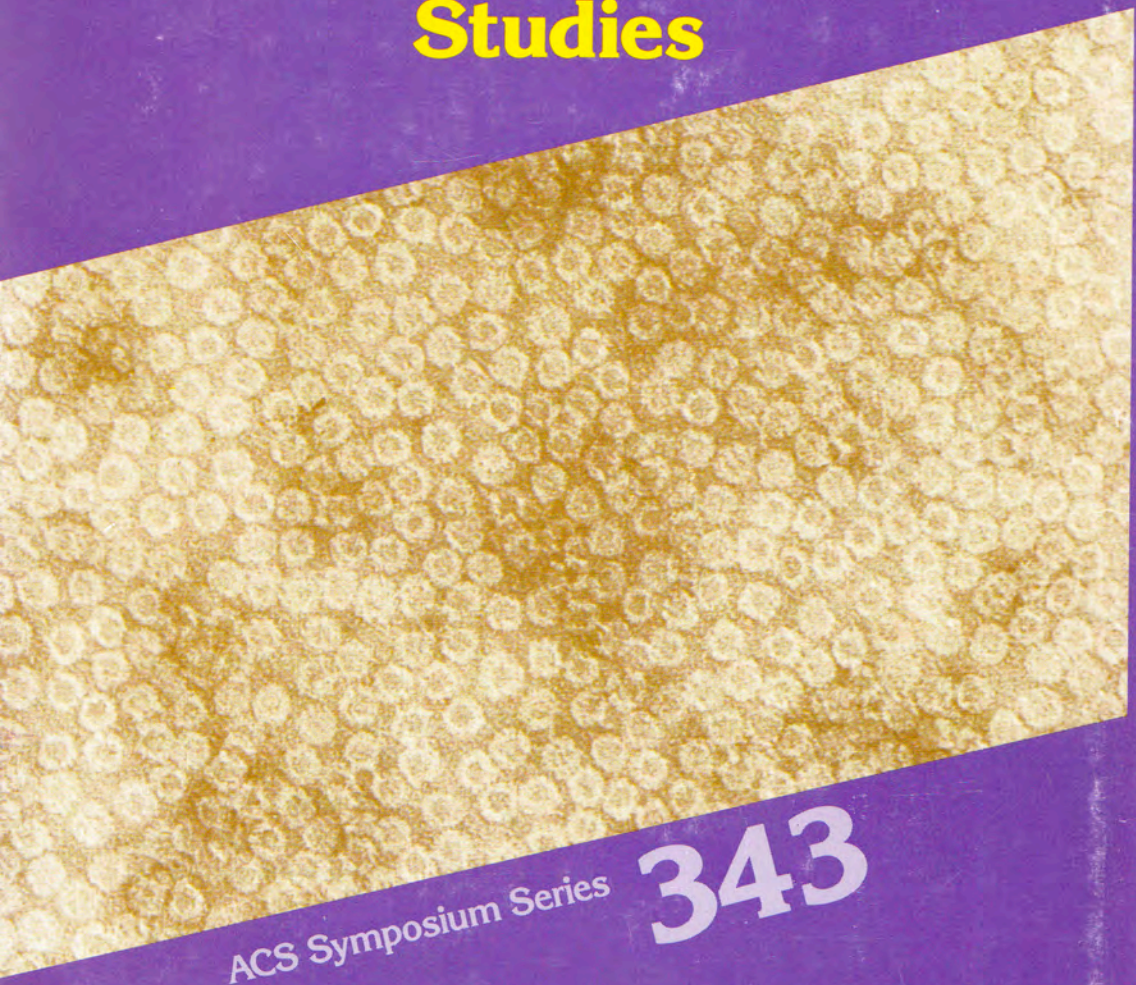

ACS Symposium Series 343

EDITED BY
John L. Brash and
Thomas A. Horbett

ACS SYMPOSIUM SERIES 343

Proteins at Interfaces

Physicochemical and Biochemical Studies

John L. Brash, EDITOR
McMaster University

Thomas A. Horbett, EDITOR
University of Washington

Developed from a symposium sponsored by
the Division of Colloid and Surface Chemistry
at the 192nd Meeting
of the American Chemical Society,
Anaheim, California,
September 7-12, 1986

American Chemical Society, Washington, DC 1987

Chapter 26

Electron Tunneling Used as a Probe of Protein Adsorption at Interfaces

J. A. Panitz

Department of Cell Biology, University of New Mexico School of Medicine, Albuquerque, NM 87131

The ability of electron tunneling to detect protein adsorption on a metal surface has been investigated. Tunneling at a vacuum-metal interface is discussed. Field-electron emission tunneling experiments are reviewed; they suggest a fundamental limit on the ability of an electron tunneling microscope to probe protein adsorption at an interface, or to image the structure of a biological macromolecule.

Tunneling is a ubiquitous phenomenon. It is observed in biological systems (1), and in electrochemical cells (2). Alpha particle disintegration (3), the Stark effect (4), superconductivity in thin films (5), field-electron emission (6), and field-ionization (7) are tunneling phenomena. Even the disappearance of a *black hole* (or the fate of a multi-dimensional universe) may depend on tunneling, but on a cosmological scale (8-9).

Classical physics dictates that a particle constrained by an energy barrier can become free only if it acquires an energy greater than the height of the barrier. In quantum mechanics, this restriction is eased. For example, quantum mechanics allows an electron to escape from the interior of a metal by *tunneling* through the potential barrier that confines it. The height of this barrier is called the work function of the metal (Φ). The work function is a property of a metal surface which can be locally modified by the presence of an adsorbate. For a clean metal surface, Φ= 1-6 eV

When a potential difference is applied to two metal electrodes in high vacuum, two types of tunneling can be observed: *metal-vacuum-metal* tunneling when the electrodes are separated by 1-2nm, or *field-electron emission* tunneling when the gap is much larger. In practice, it is difficult to measure a tunneling current in a vacuum gap when the gap is very small because the electrode spacing must be maintained without electrode contact. For this reason, the first successful tunneling experiments between closely spaced electrodes used a thin, insulating layer to define the electrode gap, and fix the electrode separation (10).

0097-6156/87/0343-0422$06.00/0

Electron Tunneling Phenomena

If all sources of conduction current in a vacuum gap are eliminated (for example, the current that would flow through an an asperity that might span the gap), a tunneling current can be observed (11-12). At small electrode separations, the tunneling current depends exponentially on both the separation of the electrodes and the work function of the cathode surface, and linearly on the voltage applied between them. A simplified, one-dimensional picture of the tunneling barrier is shown schematically in Figure 1.

If an adsorbate is placed in the tunneling gap, the tunneling current will be modified by the local change in work function that the adsorbate produces. To observe a tunneling current, electrons must tunnel from one electrode (the cathode) into the adsorbate, and then conduct through the adsorbate to the other electrode (the anode). Alternately, electrons could tunnel completely through the adsorbate, but this process becomes more improbable as the thickness of the adsorbate increases. As the adsorbate thickness increases, the electrode gap that contains it must also increase. If the adsorbate is a protein molecule, the gap must be increased to tens or hundreds of nanometers. At these distances, a tunneling current could normally not be measured.

The dimensional stability of the tunneling gap is of primary importance when proteins are placed in the gap. If the electrode separation increases, the proteins may not completely fill the gap; if the separation decreases, the proteins may be deformed or destroyed. Field-electron emission provides an alternative way to probe the tunneling properties of proteins without the difficulties imposed by small, random changes in the separation of the tunneling electrodes. Unlike metal-vacuum-metal tunneling, *field-electron emission tunneling does not explicitly depend on the separation of the electrodes in a tunneling apparatus*. As a result, large protein molecules can be placed on the cathode, and a tunneling current measured, independent of the anode position.

Field-electron emission tunneling depends exponentially on the work function of the cathode, and exponentially on the electric field strength at its surface (13). At a field strength of a few volts per nanometer, the width of the tunneling barrier will be reduced and electrons will tunnel with high probability from the cathode surface. If protein molecules are placed on the surface, the local tunneling probability will reflect their presence. Field-emitted electrons emerge as free particles in the vacuum gap, and accelerate to the anode through the potential difference that is applied across the electrodes. To avoid electrical breakdown, the electrode separation must be large, and the potential difference must be small. An easy way to generate the required field strength under these conditions is to enhance the electric field at the cathode surface by using a highly curved, needle-like cathode known as a field-emitter *tip* (See Figure 2).

A tip with the required shape and size can be prepared from fine wire by standard electropolishing techniques (14). The highly curved apex of the tip can be made smooth on an atomic scale by annealing the tip in high vacuum close to its melting point (15). Tips with an apex radius of curvature of 10-1000nm can be easily fabricated by these techniques. It is important to realize that on the scale of a single protein molecule, the highly curved apex of a large radius field-emitter tip looks like a flat surface of infinite extent.

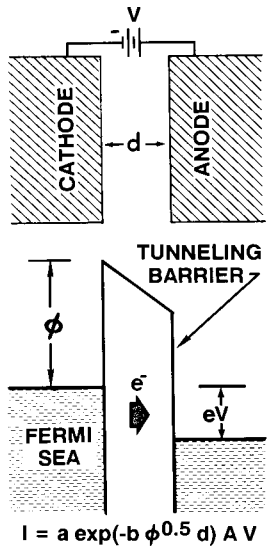

Figure 1. Metal-vacuum-metal tunneling.

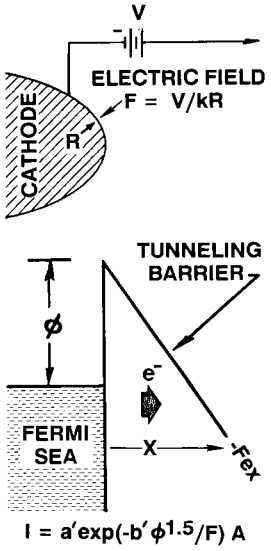

Figure 2. Field-electron emission tunneling.

Protein deposition on field-emitter tips

Reproducible deposition of protein molecules on the apex of a field-emitter tip can present formidable problems. Unlike a small organic adsorbate that can be sublimed directly onto the apex of a field-emitter tip in high vacuum, a large protein molecule must be deposited onto the tip apex from an aqueous environment, and then dried without introducing artifacts. Surface tension forces during the drying process can rearrange or distort the structure of the protein molecules adsorbed on the tip apex; proteins can even be removed from the apex as an air-liquid interface is traversed. Fortunately, the deposition problem has been solved. A surprisingly simple protocol can be used to deposit protein molecules (and most other species of biological interest) onto the apex of a field-emitter tip in a reproducible fashion (16-17).

The success of a particular deposition procedure can be determined from a series of control experiments in which the coverage of a biological species on the tip surface is determined by imaging the tip profile in the transmission electron microscope (TEM). Isolated species on the tip surface can be visualized if they are stained with uranyl acetate, or coated with a thin layer of tungsten prior to imaging (18). For example, figure 3 shows tobacco mosaic virus particles deposited from aqueous solution onto a large radius, tungsten field-emitter tip. The enzyme-cleaved virus particles were rotary shadowed with tungsten prior to imaging the tip apex in the TEM (19).

Field-electron emission Microscopy

A field-emitter tip has a unique advantage when used as the cathode in a tunneling apparatus: the electron tunneling probability at the tip apex can be directly visualized in the *field-electron emission microscope* (20). Electrons that tunnel from the apex of a field-emitter tip emerge as free particles in vacuum, and are accelerated along electric field lines that rapidly diverge into space. In the field-electron emission microscope (FEEM), the anode of a tunneling apparatus is coated with a suitable phosphor and placed far from the tip apex. The tunneling electrons that strike the phosphor form a highly magnified image that reflects their point of origin at the tip apex. Bright regions in the image reflect regions of increased electron tunneling; dark regions reflect a decrease in the electron tunneling probability.

The magnification of an FEEM image is determined by the radius of the tip apex and the distance between the tip and the phosphor-coated anode that displays the image. In practice, a magnification of several hundred thousand times is easily achieved (21). The resolution of an FEEM image is about 2nm; it is limited by the lateral velocity component of the tunneling electrons as they emerge from the tunneling barrier, and by the Heisenberg uncertainty principle that ultimately obscures their precise point of origin on the tip apex (22). Unlike other electron microscopes, the FEEM is a very simple device. Image quality is not affected by external vibrations, and high contrast images are stable for long periods of time. It has been noted that *in the absence of lenses, illuminating devices, and automatic controls a field-emission microscope is less of an apparatus and more of a direct aid to the eye and brain* (23).

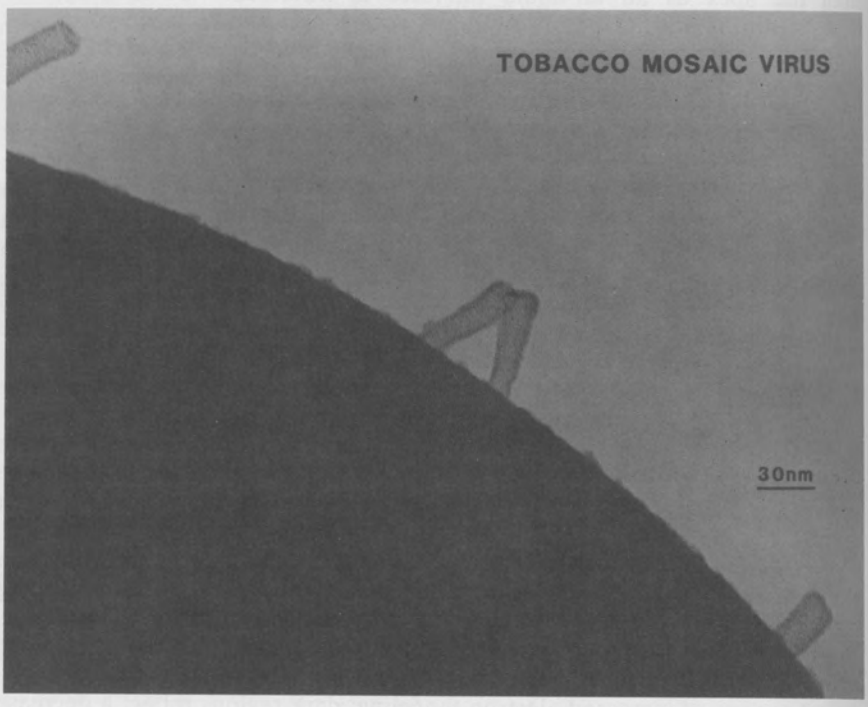

Figure 3. Transmission electron microscopy of enzyme-cleaved, tobacco mosaic virus particles on the apex of a tungsten field-emitter tip (imaged at 200kV). TMV sample kindly supplied by P. J. Butler, the MRC, Cambridge, England.

FEEM imaging of small organic molecules

Many small organic molecules can be conveniently imaged in the FEEM because they can be directly sublimed onto the apex of a field-emitter tip without sacrificing the high vacuum environment of the microscope. The first attempt to image such molecules in the FEEM was made in 1950 (24-25). Two planar molecules were studied: copper-phthalocyanine (a four-fold symmetric molecule), and flaventhrene (a two-fold symmetric molecule). Figure 4A is an FEEM image that is characteristic of a clean, (110)-oriented tungsten field-emitter tip. The symmetry of the image reflects the symmetry of the tip apex about the axis of the wire from which it was made (a result of the electropolishing technique mentioned above). Figure 4B shows the result of subliming copper phthalocyanine molecules onto the tip apex. Figure 4C shows an FEEM image of another tungsten tip exposed to the same flux of molecules for a greater time (resulting in an increased coverage of molecules on the tip apex). Figure 4D shows the result of subliming flaventhrene onto a different tungsten tip. The bright features that appear after sublimation reflect a decrease in the local work function of the surface at each adsorption site. Although these regions seem to reflect the known symmetry of each adorbate, the correspondence may be fortuitous: three-fold symmetric adsorbates (and other non-symmetric molecules) also produce two-fold and four-fold symmetric FEEM images, and other unique shapes have also been reported (26).

The symmetry of a phthalocyanine or a flaventhrene image feature is thought to reflect a complex scattering phenomenon within the molecule. The potential well defined by the molecule may tend to open a window, or *aperture*, in the tunneling barrier at the cathode surface, increasing the tunneling current at the adsorption site (27). Tunneling electrons, elastically (and inelastically) scattered from the aperture, then reemitted into space, could produce the patterns that are observed (28). Careful experiments have demonstrated that an FEEM image can accurately reflect the adsorption of a single organic molecule on the tip apex, but will not necessarily reflect its true shape or size (29).

The size of a molecular image feature in Figure 4 is about an order of magnitude larger than the size of the molecule that produced it. The increase in local image magnification has been explained by assuming that a molecule acts like a small metallic protrusion on the tip apex (30). A small metallic protrusion will distort the trajectories of the tunneling electrons in its vicinity, causing them to diverge more rapidly into space. If a molecule contains a number of quasi-free (i.e. pi) electrons, the electric field in the vicinity of the molecule will tend to be excluded from its interior, and the molecule will act like a small metallic protrusion. Although some molecules may behave in this way (e.g. semiconducting phthalocyanines), others may behave more like an insulator than a metal. The electric field will penetrate almost completely into the interior of an insulating (dielectric) protrusion. Electron trajectories in the vicinity of the protrusion will be relatively undisturbed by its presence, and the local magnification at the site of the protrusion will not change by an appreciable amount.

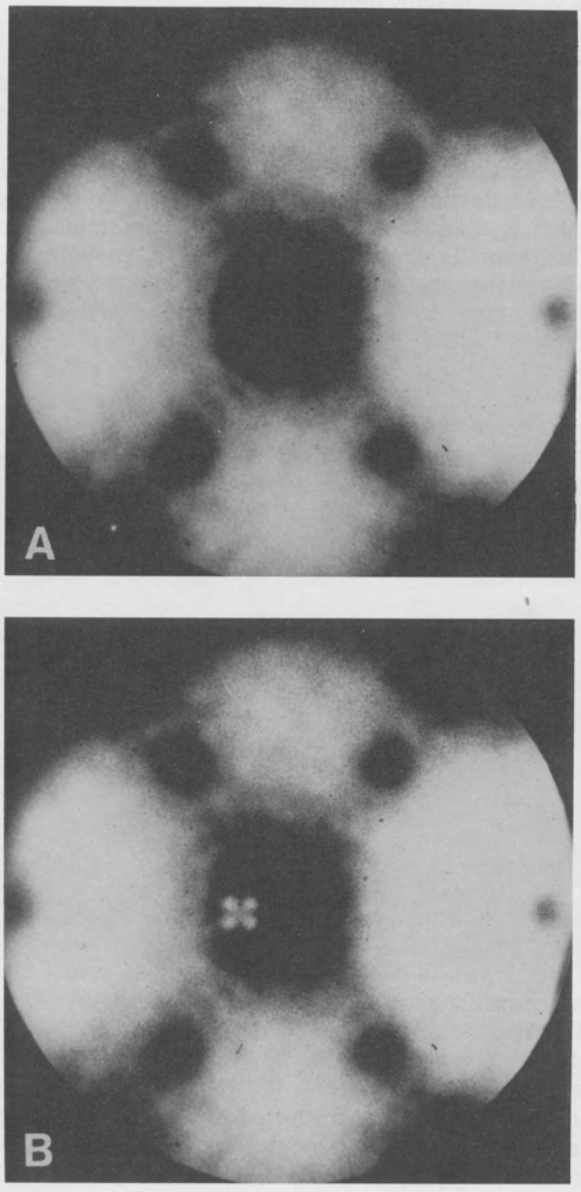

Figure 4. Field-electron emission microscopy of small, organic adsorbates. (A) 110-oriented tungsten tip. (B) With copper-phthalocyanine adsorption.

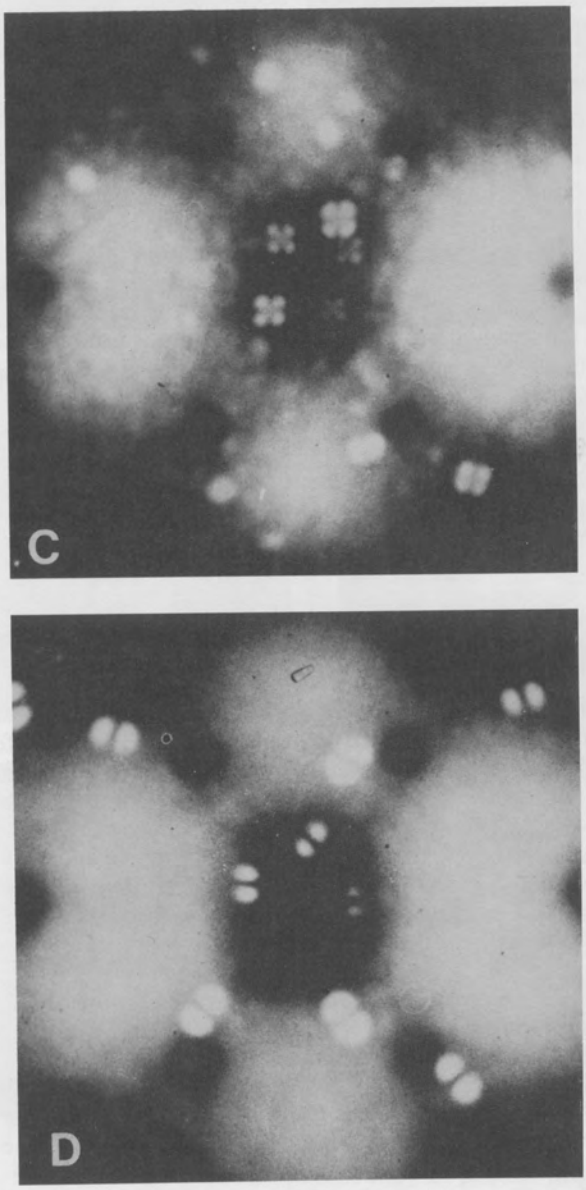

Figure 4.—*Continued*. Field-electron emission microscopy of small, organic adsorbates. (C) With increased copper-phthalocyanine. (D) With flaventhrene adsorption. (Courtesy of Dr. A. J. Melmed, The National Bureau of Standards, Gaithersburg, MD.)

FEEM imaging of Immune Complexes

The tunneling characteristics of protein molecules and virus particles have been studied by observing how they affect the appearance of an FEEM image. These experiments highlight the difficulty in handling biological species that must be removed from an aqueous environment for examination in an FEEM under ultra-high vacuum conditions. To insure some semblance of statistical reliability, many tips must be examined under reasonably identical conditions. With this in mind, thirty or forty tips are usually examined, divided into groups, with two tips in each group. One tip in each group is called the *active* tip; it is exposed to buffer containing the immune complex. The other tip is called the *control* tip; it is transferred with the active tip, in and out of the FEEM, during each stage of the imaging protocol. The control tip is used to assess the effect of tip contamination by adsorbed gas or impurities from laboratory ambient (31).

It is instructive to review the imaging protocol that was developed for studying the tunneling characteristics of ferritin/goat anti-rabbit IgG conjugate because this protocol illustrates the type of control that is required for examining any biological species in the FEEM:

(1) Two tips were cleaned by repeated heating in vacuum to 2100C. The heating schedule was designed to remove contaminant species from the tip apex by thermal desorption.

(2) An FEEM image of each tip was taken without breaking vacuum to record the field-electron emission pattern of the clean tip surface (Figure 5A and 5D).

(3) Both tips were transferred into laboratory ambient. The *active* tip was placed for 180s into an aqueous solution of 20mM Tris-Cl buffer containing 150mM NaCl at pH 7.6. The tip was rinsed in distilled water, transferred wet into a mixture of 90% ethanol in water for fifteen seconds, and then dried in air. The *control* tip remained in laboratory ambient during this time.

(4) Both tips were returned to the vacuum system and an FEEM image was taken of each tip after a 12 hour pumpdown (Figure 5B and Figure 5E). The bright features in Figure 5B are characteristic of exposing a tip to an aqueous solution of buffer (that does not contain protein molecules) as described above.

(5) Both tips were transferred into laboratory ambient. The *active* tip was placed in buffer containing ferritin/IgG conjugate at a concentration of about 12.5 micrograms/ml. After three minutes the *active* tip was rinsed as described in (3), above. Previous TEM images confirmed that this procedure resulted in a saturation coverage of the immune complex on the tip surface. The *control* tip remained in laboratory ambient during the deposition procedure.

(6) Both tips were returned to the vacuum system, and an FEEM image was taken of each tip. The image of the *active* tip (Figure 5C) reflects the adsorption of gas phase contaminants during tip transfer in air, the adsorption of buffer molecules, and the adsorption of ferritin/IgG complexes from solution. The total tunneling current from a tip exposed to the protein complex is greatly reduced (or eliminated) when compared to the tunneling current from a clean tip, or a control tip (Figure 5F).

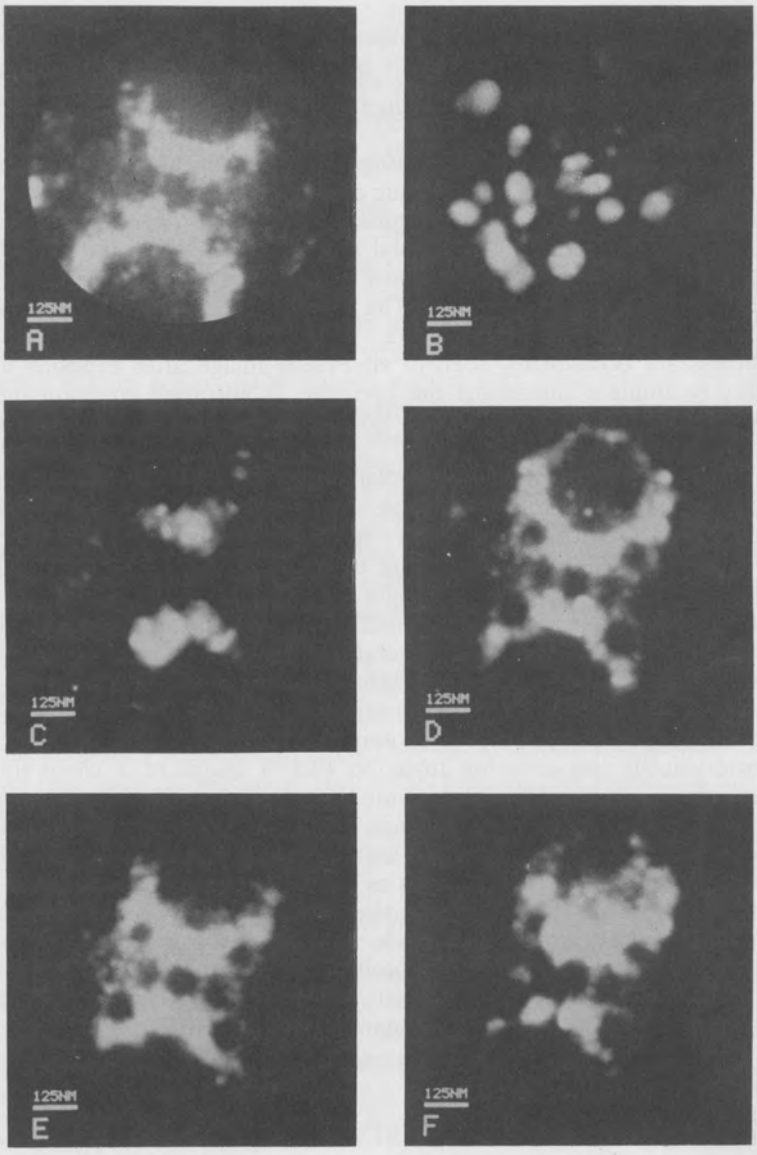

Figure 5. Field-electron emission microscopy of protein adsorbates. (A) Active tip prior to deposition. (B) Deposition in buffer without ferritin-IgG. (C) Deposition in buffer with ferritin-IgG. (D) Control tip prior to air exposure. (E) After exposure to laboratory ambient. (F) After subsequent exposure to laboratory ambient. (Reproduced with permission from Ref. 31. Copyright 1984 The American Institute of Physics.)

Conclusions

As a result of the FEEM imaging experiment described above, and other (unpublished) FEEM experiments, the following general conclusions have been reached:

(1) Repeated exposure of a tungsten tip to laboratory ambient does not seem to appreciably alter its tunneling characteristics. Since the tip apex must be covered with a monolayer of gas phase contaminants (as a result of exposure to laboratory ambient), the adsorbed species must either not affect FEEM image contrast, or the adsorbates must desorb from the tip surface during the pumpdown cycle prior to imaging. The latter effect is probably responsible for the image contrast that is observed. Localized regions of increased image brightness are occasionally seen in an FEEM image after exposing a tip to laboratory ambient (indicating the presence of adsorbed contaminants), but these features are short lived and do not survive minor increases in field strength (of the order of 0.5%).

(2) If a clean tip is exposed to buffer (the type of buffer does not seem to matter), a characteristic FEEM image is recorded in vacuum. Image features consist mainly of bright, circular regions of increased contrast, often superimposed on a weak background image that looks similar to an FEEM image of a clean tip. Unlike the bright regions that are occasionally observed in a control tip image after air exposure, these bright regions are stable, even if the imaging field is increased by several percent. The increased emission has been correlated with the presence of salt in the buffer solution.

(3) The FEEM image of a tip exposed to an aqueous solution of buffer containing a protein (the exact protein appears to be unimportant) shows characteristically less emission than the FEEM image of a clean tip, or a control tip. Electron tunneling from large regions of the tip surface is suppressed, apparently by the presence of protein molecules in these regions. The reduction in the total emitting area is in qualitative agreement with the coverage of protein on the tip apex as judged by subsequent imaging in the TEM (unpublished). We interpret these observations by suggesting that a protein molecule behaves like a thick, insulating protrusion on the tip apex. Tunneling seems to occur with high probability only from the regions of the tip apex that are not covered with protein. Precise, *probe-hole* measurements of the tunneling current are needed to quantify this effect (32).

Implications for STM imaging

The scanning tunneling microscope (STM) is a high resolution, non-contacting, surface profilometer (33). Contrast is generated in an STM image by mapping the tunneling probability of electrons across a surface scanned by a field-emitter tip. A tip is used to limit and define the tunneling region of the surface. As the tip is rastered within 1nm of the surface (by piezoelectric crystals), a metal-vacuum-metal tunneling current is recorded. The tunneling current is kept constant as the tip scans the surface by allowing the tip to move vertically with respect to the surface below. A plot of raster position verses tip elevation records the surface profile in three dimensions. STM images of semiconductor surfaces show structure at the atomic level, but the appearance of an image

depends on the bias voltage that is applied between the tip and the surface (34-35). The STM has also been used to image unstained virus particles in laboratory ambient, but the images have not been reproduced and are unconvincing when compared to their TEM counterparts (36). STM images of fatty acid bilayers deposited by the Langmuir-Blodgett technique and imaged in air have also been reported (37).

Unstained protein molecules, and unstained virus particles (unpublished results), do not image in the FEEM. Tunneling appears to be negligible or absent at the adsorption site of these species. STM images reflect a reasonably large tunneling probability for these species; FEEM images do not, and the dichotomy is puzzling. Field-electron emission images are consistent with a picture of a protein molecule (or a virus particle) that behaves like a large, insulating species while STM images suggest that these species are at least quasi-conductors for the tunneling electrons. Perhaps the different degree of hydration of the species that result from the two imaging techniques may account for the different tunneling characteristics that have been reported (FEEM images of biological species must be produced in a high vacuum environment while STM images can be taken in laboratory ambient). More complete studies of electron tunneling through protein molecules under a variety of deposition and imaging conditions will be needed to resolve the fundamental questions that have been raised by these two types of tunneling experiments.

Acknowledgment

The author wishes to acknowledge the Defense Advanced Research Projects Agency (Advanced Biochemical Technology Program) for supporting this research under ARPA contract 4597.

Literature Cited

1. Frauenfelder, H. In *Tunneling in Biological Systems*; Chance, B., Ed.; Academic Press: New York, 1979; p 627.
2. Gurney, R. W. *Proc. R. Soc. London.* 1932, **A134**, 137.
3. Gamow, G. *Z. Phys.* 1928, **51**, 204.
4. Lanczos, C. Z. *Z. Phys.* 1931, **68**, 204.
5. Giaever, I.; In *Tunneling Phenomena in Solids*; Plenum: New York, 1969; Chapter 19.
6. Eyring, C. F.; Mackeown, S. S.; Millikan R. A. *Phys. Rev.* 1928, **31**, 900-09.
7. Inghram, M. G.; Gomer, R. *J. Chem. Phys.* 1954, **22**, 1279-82
8. Page, D. N. *Nature.* 1986, **321**, 111.
9. M. J. Perry. *Nature.* 1986, **320**, 679.
10. Giaever, I.; *J. Appl. Phys.* 1961, **32**, 172-77.
11. Teague, E. C. *Bull. Am. Phys. Soc.* (March) 1978, **23**, 290
12. Binnig, G.; Rohrer, H.; Gerber, Ch.; Weibel, E. *Appl. Phys. Lett.* 1982, **40**, 178-80.
13. Fowler, R. H.; Nordheim, L. W. *Proc. R. Soc. London.* 1928, **A119**, 173.

14. Muller, E. W.; Tsong, T. T. *Field-Ion Microscopy: Principles and Applications*. Elsevier: New York, 1969; p 119-27.
15. Boling, J. L.; Dolan, W. W. *J. Appl. Phys.* 1958, **2**, 556-59.
16. Panitz, J. A.; Andrews, C. L.; Bear D. G. *J. Elec. Micros. Techn.* 1985, **2**, 285-92.
17. Panitz J. A. *Rev. Sci. Instrum.* 1985, **56**, 572-74.
18. Panitz, J. A. In *Science of Biological Specimen Preparation*; Muller, M; Becker, R. P.; Boyde, A.; Wolosewick, J. J., Eds.; SEM Inc.: AMF O'Hare (Chicago), 1985; p 283.
19. Panitz, J. A.; Bear, D. G. *J. Micros. (Oxford)*. 1985, **138**, 107-10.
20. E. W. Muller. *Z. Physik.* 1937, **106**, 541-50.
21. Panitz, J. A. In *Methods of Experimental Physics*; Park, R. L.; Lagally, M, Eds.; Academic: New York, 1985; Vol. 22, Chapter 7.
22. Gomer, R. *Field Emission and Field Ionization*; Harvard Press: Cambridge, 1961; Chapter 2.
23. Rochow, T. G.; Rochow, E. G. *An Introduction to Microscopy by Means of Light, Electrons, X-rays, or Ultrasound*; Plenum: New York, 1978; p 35.
24. E. W. Muller. *Naturwissenschaften*. 1950, **14**, 333.
25. E. W. Muller. *Life*. (June) 1950, **28**, 67.
26. E. W. Muller. *Ergebnisse d. exakt. Naturwiss.* 1953, **27**, 290-360.
27. Gomer, R. *Field Emission and Field Ionization*; Harvard Press: Cambridge, 1961; Chapter 5.
28. Gadzuk, J. W.; Plummer, E. W. *Rev. Mod. Phys.* 1973, **45**, 487-548.
29. Melmed, A. J.; Muller, E. W. *J. Chem. Phys.* 1958, **186**, 1037.
30. D. J. Rose. *J. Appl. Phys.* 1956, **27**, 215-20.
31. Panitz, J. A. *J. Appl. Phys.* 1984, **56**, 3319-23.
32. Muller, E. W. *Z. Phys.* 1943, **120**, 261, 270.
33. Quate, C. F. *Physics Today*. (August) 1986, **86**, 26-33.
34. Golovchenko, J. A. *Science*. 1986, **232**, 48-53.
35. Hamers, R. J.; Tromp, R. M.; Demuth, J. E. *Phys. Rev. Letts.* 1986, **56**, 1972-75.
36. Baro, A. M.; Miranda, R.; Alaman, J.; Garcia, N.; Binnig, G.; Rohrer, H.; Gerber, Ch.; Carrascosa, J. L. *Nature*. 1985, **315**, 253-54.
37. Rabe, J.; Gerber, Ch.; Swalen, J. D.; Smith, D. P. E.; Bryant, A.; Quate, C. F. *Bull. Am. Phys. Soc.* (March) 1986, **31**, 289.

RECEIVED February 18, 1987